Carbohydrate Polymers 94 (2013) 221–228

Contents lists available at SciVerse ScienceDirect

Carbohydrate Polymers

journal homepage: www.elsevier.com/locate/carbpol

Synthesis, physiochemical and optical properties of chitosan based dye containing naphthalimide group

Santosh Kumar, Joonseok Koh*

Department of Organic and Nano System Engineering, Konkuk University, 120 Neungdong-ro, Gwangjin-gu, Seoul 143-701, Republic of Korea

ARTICLE INFO

Article history:
Received 15 September 2012
Received in revised form
20 December 2012
Accepted 8 January 2013
Available online 16 January 2013

Keywords:
N-naphthaloyl chitosan
Chitosan biopolymer dye
Optical property
Biomedical

ABSTRACT

A new biopolymer dye containing naphthalimide moiety was synthesized by reaction of *N*-naphthaloyl chitosan with 1-ethyl-6-fluoro-1,4-dihydro-4-oxo-7-piperazino-3-quinolinecarboxylic acid. *N*-naphthaloyl chitosan was synthesized by reaction of chitosan with 4-bromo-1,8-naphthalic anhydride in aqueous media by greener approach. The degree of substitution of chitosan biopolymer dye is 0.55 with a yield of 70%. The synthesized materials were characterized by using UV–vis, ^{1}H NMR, FTIR, and FT-Raman spectroscopy. Some physical properties and surface morphology were characterized by X-ray diffraction (XRD), thermogravimetric analysis (TGA), differential scanning calorimetry (DSC) and scanning electron microscopy (SEM). Optical properties of chitosan biopolymer dye were evaluated by photoluminescence (PL) spectroscopy that showed red shift (λ_{em}) peak at 442 nm and 551 nm at excitation wavelength 325 nm in comparison to chitosan. The solubility of chitosan biopolymer dye increased in most of the organic solvents. These results may provide new perspectives in biomedical applications as an optical and sensitive biosensor material.

1. Introduction

The fluorescent biomaterials have been the focus of intense research focus in optoelectronic devices and applications of biological fields such as in cellular imaging, biosensing, biomedical, gene delivery and drug delivery (Jang, Bae, & Park, 2006; Lim, Kim, Kwon, Ahn, & Park, 2009; Michalet et al., 2005; Seydack, 2005). Fluorescence techniques have been widely used and are still enjoying ever-increasing interest from chemistry to many areas of biology due to high sensitivity, simplicity, fast response, a wealth of molecular information, and capability of spatial imaging. However, the feasibility of using fluorescence techniques for a particular application is often limited by the availability of appropriate fluorescent molecules. Although there have been some reports about theoretical approaches for the rational design of fluorescent probes, these are still far from enough. Combinatorial construction of libraries of fluorescent probe candidates has been demonstrated to be a very powerful and promising approach with some impressive discoveries of novel fluorescent probes.

Naphthalimide derivatives have been used as supramolecular moieties for the study of photo-induced electron transfer. It exhibits excellent photostability, high fluorescence quantum yields, electron accepting abilities and sensory applications. Naphthalimide derivatives have also shown promise in bio-related research fields (Lee et al., 2012; Wang et al., 2012; Zhang et al., 2011), organic light emitting diodes (Coya et al., 2012), nonlinear optical (Zhang et al., 2002), dye-sensitised solar cells (Huang, Fang, Li, Xie, & Zhu, 2011), electroluminescent materials (Zhu, Minami, Kazaoui & Kim, 2003) and extensively used as strongly absorbing dyes in the dye industry (Bojinov, Ivanova, & Simeonov, 2004). Recently, Lee et al. have demonstrated galactose appended naphthalimide of targetable ligand for hepatic thiol imaging in living cells and animals (Lee et al., 2012).

Of late, focus of researchers in the fluorescent biomaterials have been shifted to fluorescent organic dyes; fluorescent proteins and quantum dots having strong fluorescence, high photo-stability, broad excitation spectra, long fluorescence lifetime and narrow emission spectra, however cytotoxicity and environmental concerns limits its applications. Therefore, it is an important challenge to search for environmental friendly fluorescent materials. Biomaterials have been attracting wide attention as they show much more stable emissions, lower cytotoxicity and give rise to less environmental concern. Yang et al. reported highly amino-functionalized fluorescent carbon nanoparticles fabricated by hydrothermal carbonization of chitosan at a mild temperature (Yang et al., 2012).

Chitin is a material which is being used in diversified field of research. Chitosan manufactured from chitin, is the linear and partly acetylated (1–4)-2-amino-2-deoxy-β-D-glucon (Muzzarelli, 1977; Muzzarelli et al., 2012). Chitosan is nontoxic, biofunctional, biodegradable, and biocompatible and can be used as biomedical applications (Muzzarelli & Muzzarelli, 2005). Recently, hydrophobically modified chitosan is reported having

* Corresponding author. Tel.: +82 2 3437 0238; fax: +82 2 3437 0238.
E-mail address: ccdjko@konkuk.ac.kr (J. Koh).

0144-8617/$ – see front matter © 2013 Elsevier Ltd. All rights reserved.
http://dx.doi.org/10.1016/j.carbpol.2013.01.011

representative examples that hold considerable potential as drug carriers and bioimaging agents due to high biocompatibility and high tumor targeting efficiency (Kim et al., 2005; Lim et al., 2009; Lim, Shin, Kwon, Jeong, & Kim, 2012). Chitosan combined with dye molecules can enhance fluorescence, which is also helpful to increase the sensitivity and decrease the consumption of probe molecules (Wang et al., 2006). 1-Ethyl-6-fluoro-1,4-dihydro-4-oxo-7-piperazino-3-quinolinecarboxylic acid (norfloxacin) possesses antibacterial activity belonging to the group of fluoroquinolones. It inhibits the enzyme DNA gyrase and protein synthesis (Katsarou, Efthimiadou, Psomas, Karaliota, & Vourloumis, 2008). It is used in the treatment of gonorrhea, prostrate and urinary tract infections (Mazuel, 1991). Norfloxacin has been studied with respect to its binding to calf thymus DNA using fluorescence and linear dichroism techniques (Son et al., 1998). Dizman et al. have synthesized methacrylate polymers containing norfloxacin for antibacterial activities (Dizman, Elasri, & Mathias, 2005). The introduction of naphthalimide and fluoroquinolone moieties to chitosan biopolymer can provide excellent electro- and photo-active properties.

This paper aims to synthesize and characterize, fluorescence based chitosan biopolymer dyes. This material may play a role in the biomedical applications, in vitro and in vivo diagnostics, and in the screening of new potential drug agents.

2. Experimental

2.1. Materials and reagents

The chitosan powder was purchased from product of Qingdao Yunzhou Biochemistry Co. Ltd. China, and a degree of deacetylation (DD) of 95%. 4-Bromo-1,8-naphthalic anhydride (Sigma–Aldrich), 1-ethyl-6-fluoro-1,4-dihydro-4-oxo-7-piperazino-3-quinolinecarboxylic acid (Fluka), DMF (Samchun Chemicals, Korea), anhydrous potassium carbonate (Yakuri Pure Chemicals Co. Ltd, Kyoto, Japan), hydrochloric acid (Samchun Chemicals, Korea), and glacial acetic acid (Dae Jung, Korea) were used without further purification. The purity of synthesized compounds has been checked by TLC using silica gel with different solvent systems.

2.2. Characterization

Fourier transform infrared (FT-IR) spectroscopic measurements were performed using a JASCO FT-IR. FT Raman spectra were recorded on a Bruker MultiRam spectrometer (Bruker) with Ge diode as detector that is cooled with liquid-nitrogen. A cw-Nd:YAG laser (λ = 1064 nm) was used as excitation source. The spectra were recorded over 3500–0 cm^{-1} using spectral resolution of 4 cm^{-1} and a laser power output of 100 mW. ^{1}H NMR spectra were recorded in a Bruker 600 MHz NMR spectrometer using tetramethylsilane (TMS) as the internal standard and DMSO-d_6 as a solvent. Thermogravimetric analysis (TGA) was carried out in a TA Q 50 system TGA. The samples were scanned at a heating rate of 10 °C/min under flow of nitrogen. Differential scanning calorimetry (DSC) with DSC Q1000V7.0 Universal V3.6C TA instrument in aluminum pans, heating and cooling rates of 10 °C/min was used. Identification and quantitative determination of the various crystalline phases were studied using X-ray diffractometer (D/Max2500VB+/Pc, Rigaku, Japan) with Cu Kα characteristic radiation (wavelength λ = 0.154 nm) at a voltage of 40 kV and a current of 50 mA. The scanning rate was 3°/min and the scanning diffraction angle 2θ was between 2° and 40° at room temperature (25 °C). The surface morphology was analyzed by scanning electron microscopy JEOLJSM-6490LA. The solubility of chitosan and chitosan biopolymer dye in different solvents were examined. UV–visible absorption spectra were measured in 1 cm quartz cells on an Agilent 8453 spectrophotometer (USA). The photoluminescence (PL) spectra were recorded on a Perkin-Elmer LS55 fluorescence spectrometer.

2.3. Synthesis

2.3.1. Synthesis of N-naphthaloyl chitosan (**2**)

N-naphthaloyl chitosan was synthesized by greener approach according to the literature (Ifuku, Miwa, Morimoto, & Saimoto, 2011). In a round bottom flask (50 mL) chitosan (0.6 g, 0.0018 mol) and 4-bromo-1,8-naphthalic anhydride (1.529 g, 0.0055 mol) in 20 mL of 1% of glacial acetic acid was refluxed at 120 °C for 28 h. After cooling at room temperature, the precipitate was collected by centrifugation and filtration, followed by thorough washing with deionized water and ethanol. The synthesized material was dried at 85 °C under reduced pressure to give a product. For complete dehydration of the partial amide moiety (*N*-(2-carboxy)benzoyl group), *N*-naphthaloyl chitosan was heated at 190 °C in vacuo for 5 h (Satoh, Vladimirov, Johmen, & Sakairi, 2003).

2.3.2. Acetylation of N-naphthaloyl chitosan

N-naphthaloyl chitosan was acetylated for NMR measurements. In round bottom flask (50 mL) *N*-naphthaloyl chitosan (0.1 g) was suspended in 5 mL of pyridine and added into 2.5 mL of acetic anhydride under stirring at 100 °C for 24 h. The contents were poured into methanol. The precipitate was filtered, washed with ethanol, and dried at 45 °C in vacuo.

^{1}H NMR (600 MHz, DMSO-d_6) δ (ppm) 8.62–8.57 (q, 1H, naphthalimide, H-5), 8.55 (t, 1H, naphthalimide, H-7), 8.39 (d, 1H, naphthalimide, H-2), 7.80–7.77 (d, 1H, naphthalimide, H-6), 7.39–7.37 (m, 1H, naphthalimide, H-3), 5.76 (s, H-1 of GlcNAc unit), 4.37 (br s, H-1 of GlcN unit), 3.61–4.03 (br m, H-3, 4, 5,6 of GlcN unit; and H-2, 3, 4, 5,6 of GlcNAc unit), 3.34 (br s, H-2 of GlcN residue), 2.50 (br s, NH_2 and $NHCOCH_3$). DS = 0.55.

2.3.3. Synthesis of chitosan biopolymer dye (**3**)

In a three necked round bottom flask (100 mL) *N*-naphthaloyl chitosan (0.650 g, 0.001 mol), 1-ethyl-6-fluoro-1,4-dihydro-4-oxo-7-piperazino-3-quinolinecarboxylic acid (0.31 g, 0.001 mol) and 1.5 equiv. of anhydrous K_2CO_3 (0.207 g, 0.0015 mol) in dry DMF (15 mL) was heated rapidly to 110 °C and refluxed for 1 h under nitrogen atmosphere. After cooling, the contents were poured into aqueous hydrochloric acid, filtered and dried at room temperature to give a yellow solid of chitosan biopolymer dye with a yield of 70%.

2.3.4. Acetylation of chitosan biopolymer dye

This procedure is similar with the aforementioned methodology for chitosan polymer dye. Chitosan biopolymer dye was acetylated for NMR measurements. In round bottom flask Chitosan polymer dye (0.1 g) was suspended in 5 mL of pyridine and treated with 3 mL of acetic anhydride under stirring overnight at 100 °C, the polymer was precipitated into methanol, filtered washed with ethanol, and dried at 45 °C in vacuo.

^{1}H NMR (600 MHz, DMSO-d_6) δ (ppm) 9.01 (s, 1H, fluoroquinolone, H-2), 8.62 (q, 1H, naphthalimide, H-5), 8.48 (d, 1H, naphthalimide, H-7), 8.39 (d, 1H, naphthalimide, H-2), 8.01 (d, 1H, naphthalimide, H-6), 7.79 (t, 1H, naphthalimide, H-3), 7.49 (d, 1H, fluoroquinolone, H-6), 7.37 (d, 1H, fluoroquinolone, H-8), 5.76 (s, H-1 of GlcNAc unit), 4.66–4.64 (broad, quinolone N—CH_2), 4.38 (br s, H-1 of GlcN unit), 3.68 (d, 8H, piperazine), 3.61–4.03 (br m, H-3, 4, 5, 6 of GlcN unit; and H-2, 3, 4, 5, 6 of GlcNAc unit), 3.35 (br s, H-2 of GlcN residue), 2.50 (br s, NH_2 and $NHCOCH_3$), 1.59 (t, 3H, —CH_3). DS = 0.55.

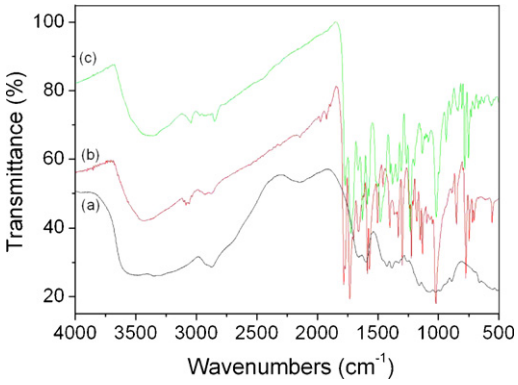

Fig. 1. FTIR of chitosan (a), *N*-naphthaloyl chitosan (b) and chitosan biopolymer dye (c).

3. Results and discussion

Our approach for the modification of chitosan biopolymer via Green synthesis is one of the most important concerns in environmental aspects and biomedical applications (Scheme 1). It is generally accepted that natural dyes are more eco-friendly and safer than synthetic dyes. Identification of the synthesis of chitosan biopolymer dye was confirmed by FTIR, FT-Raman and ^{1}H NMR.

3.1. FTIR spectroscopy

Identification of the synthesis of *N*-naphthaloyl chitosan and chitosan biopolymer dye was confirmed by FTIR. The FTIR spectra of chitosan, *N*-naphthaloyl chitosan and chitosan biopolymer dye are shown in Fig. 1a, b and c respectively. The FTIR characteristic peaks of pure chitosan (Fig. 1a) absorption peaks at 3360 cm^{-1} due to O—H stretched overlapped with N—H stretch, 2919 and 2874 cm^{-1} due to C—H stretch, 1640 cm^{-1} due to amide II band C—O stretch of acetyl group, 1592 cm^{-1} amide II band of N—H stretch, 1420–1377 cm^{-1} (asymmetric C—H stretch bending of CH_2 group and 1061 cm^{-1} was assigned to skeletal vibration involving the bridge C—O stretch of glucosamine residue (Kumar, Koh, Kim, Gupta, & Dutta, 2012). With the comparison of the spectra of chitosan, *N*-naphthaloyl chitosan and chitosan biopolymer dye, the N—H stretch at 3439–3362 cm^{-1} due to O—H stretched overlapped with N—H stretch (Kumar et al., 2012). The FTIR spectra of *N*-naphthaloyl chitosan (Fig. 1b) revealed characteristic absorption bands at 1770–1728 cm^{-1} due to the imide carbonyl naphthalamide, and absorption band at 554 cm^{-1} due to C—Br stretching. FTIR spectra of chitosan biopolymer dye (Fig. 1c) absorption bands at 1764–1723 cm^{-1} due to the imide carbonyl bond (Ghassemi & Hay, 1993). The bromine group (C—Br) disappeared in the spectra of chitosan biopolymer dye because on this position piperazine is attached, it confirms the successful substitution of the bromo group by the piperazine hydrogen of 1-ethyl-6-fluoro-1,4-dihydro-4-oxo-7-piperazino-3-quinolinecarboxylic acid at the C-4 position. The absorption peak at 1660–1625 cm^{-1} represented to N—H bending vibration of quinolones. The bands at the 1510–1472 cm^{-1} was assigned stretching vibration of O—C—O group of acid and at 1306–1260 cm^{-1} suggested bending vibration of O—H group, which indicated the presence of carboxylic acid. The strong absorption band at 1020 cm^{-1} was assigned to stretching vibration of C—F group (Sahoo, Chakraborti, Mishra, Nanda, & Naik, 2011). The intensity band OH affects on the degree of substitution which become broader on stretching and moves to a higher frequency with increasing DS up to ~80% (Singh & Dutta, 2009).

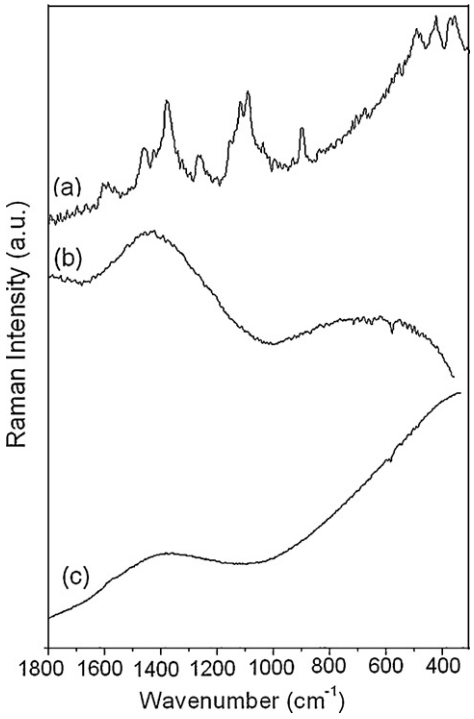

Fig. 2. FT-Raman spectra of chitosan (a), *N*-naphthaloyl chitosan (b) and chitosan biopolymer dye (c).

3.2. FT-Raman analysis

Raman spectroscopy has been a standard tool for studying characteristic vibrational modes of materials. The FT-Raman spectra of chitosan, *N*-naphthaloyl chitosan and chitosan biopolymer dye are shown in Fig. 2a, b and c respectively. Chitosan (Fig. 2a) shows a band at 1599 cm^{-1} is assigned to deformation mode of NH_2 group (Socrates, 2001; Zhang, Geissler, Fischer, Brendler, & Baucker, 2012). The Raman bands at 1460 and 1380 cm^{-1} is assigned to various deformation vibrations of polysaccharides backbones; and 1153 cm^{-1} due to the asymmetric vibration of glycosidic C—O—C groups. The band at 1117 and 1089 cm^{-1} was due to the symmetric stretching vibration of glycosidic C—O—C groups. A Raman peak at 2879 cm^{-1} was the characteristic of stretching vibration of C—H groups in glucosamine residue (not shown) (Zhang et al., 2012). The Raman spectra of *N*-naphthaloyl chitosan (Fig. 2b) revealed characteristic featured shows the 1660 cm^{-1}–1114 cm^{-1} due to the naphthalamide group (Saksena, 1938) and the bands at 689–500 cm^{-1} was the characteristic of stretching vibration of the C—Br. For the Raman spectra of chitosan biopolymer dye (Fig. 2c) has a fluorescent background so, the chromophores overlaps with the Raman signal, we could not observe clearly all the peaks. According to Raman spectra we can compare here the bromine group (C—Br) disappeared in the Raman spectra of chitosan biopolymer dye (Fig. 2c), it confirms the successful substitution of the bromo group by the piperazine hydrogen of 1-ethyl-6-fluoro-1,4-dihydro-4-oxo-7-piperazino-3-quinolinecarboxylic acid at the C-4 position.

3.3. TGA analysis

The TGA thermograms of chitosan, *N*-naphthaloyl chitosan and chitosan biopolymer dye are shown in Fig. 3. TGA of chitosan Fig. 3a showed two different stages of weight loss. The first stage weight loss starting from 47 to 100 °C, this might corresponds to the loss of adsorbed and bound water. The second stage of weight loss starts

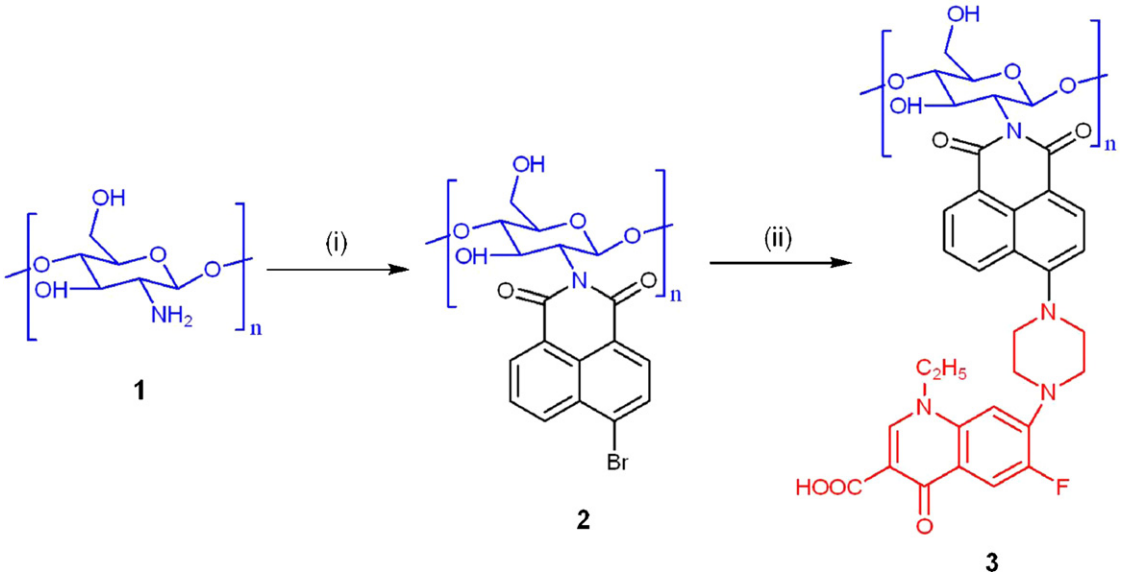

Scheme 1. Synthesis scheme for the preparation of chitosan biopolymer dye **3**. Reagents and conditions: (i) 4-bromo-1,8-naphthalic anhydride, aqueous acetic acid (1%v/v), 120 °C, 28 h; (ii) 1-ethyl-6-fluoro-1,4-dihydro-4-oxo-7-piperazino-3-quinolinecarboxylic acid, 1.5 equiv. of anhydrous K_2CO_3/dry DMF, 110 °C, 1 h under nitrogen.

at 247 °C and continues up to 330 °C due to the degradation of chitosan biopolymer (Katritzky & Narindoshvili, 2008). In Fig. 3b, observed TGA thermogram studies indicate the two weight loss, *N*-naphthaloyl chitosan began to slow weight loss at about 59 °C due to evaporation of water and moisture content in the polysaccharide. At the second stage, A fast process of weight loss appears in *N*-naphthaloyl chitosan decomposing from 191 to 308 °C, is might be due to the naphthalimide group in a polymer. The TGA thermogram studies of polymer dye Fig. 3c indicated the three different weight losses. It can be seen that Fig. 3c begins to lose weight around 172–198, 198–339 and 368–461 °C. The results demonstrate the loss of the thermal stability for chitosan biopolymer dye to the chitosan. Introduction of naphthalimide and fluoroquinolone group into polysaccharide structure may be disrupting the crystalline structure of chitosan, through the loss of the hydrogen bonding.

3.4. DSC analysis

The DSC thermograms of pure chitosan, *N*-naphthaloyl chitosan, and chitosan biopolymer dye, under nitrogen in the temperature range from 30 to 300 °C are shown in Fig. 4. The DSC of pure chitosan (Fig. 4a) showed one broad endothermic peak at 158 °C. In contrast, DSC of *N*-naphthaloyl chitosan (Fig. 4b) showed two endothermic peaks at 216 °C and 246 °C, respectively and exothermic peak at 254 °C. The DSC thermogram of chitosan derivative (Fig. 4c) represent intense endothermic peak at 190 °C and exothermic peak at 205 °C corresponding to thermal degradation of chitosan biopolymer dye. The thermal behavior of the chitosan biopolymer dye is mainly due to cleavage or degradation of norfloxacin and naphthalimide.

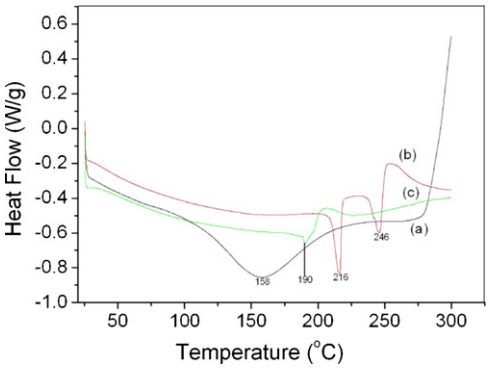

Fig. 4. DSC of chitosan (a), *N*-naphthaloyl chitosan (b) and chitosan biopolymer dye (c).

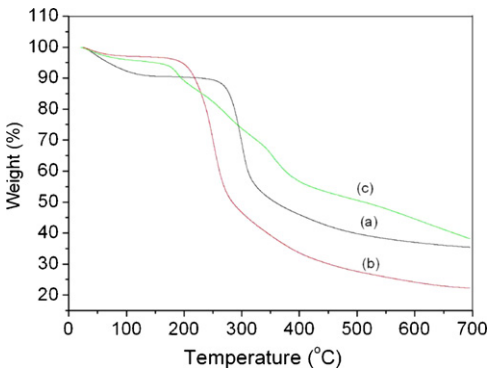

Fig. 3. TGA of chitosan (a), *N*-naphthaloyl chitosan (b) and chitosan biopolymer dye (c).

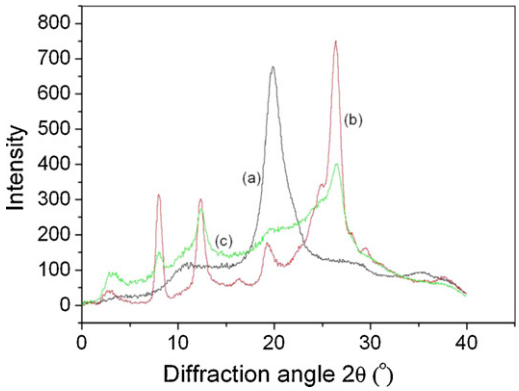

Fig. 5. XRD of chitosan (a), *N*-naphthaloyl chitosan (b) and chitosan biopolymer dye (c).

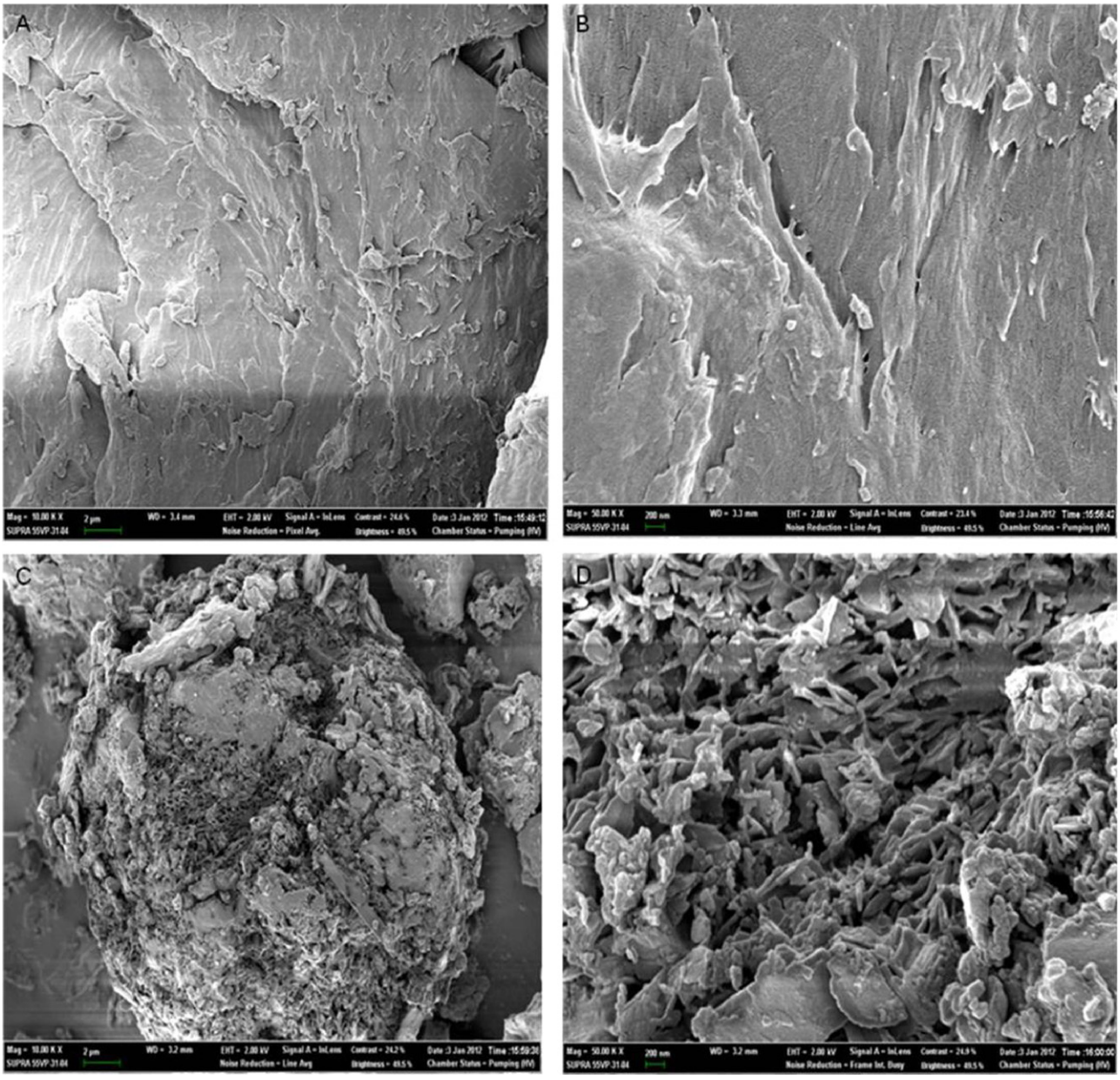

Fig. 6. SEM characterization of chitosan (A and B) and chitosan biopolymer dye (C and D).

Table 1
Solubility test of chitosan biopolymer dye in various solvents.

Solvent	Chitosan	Chitosan biopolymer dye
Petroleum ether	Insoluble	Insoluble
Water	Insoluble	Insoluble
Acetic acid (1%)	Soluble	Insoluble
DMSO	Insoluble	Soluble
Chloroform	Insoluble	Soluble
Ethyl acetate	Insoluble	Insoluble
Acetone	Insoluble	Partially soluble
Ethanol	Insoluble	Partially soluble
Acetonitrile	Insoluble	Partially soluble
N,*N*-dimethyl acetamide	Insoluble	Soluble
1,4-dioxane	Insoluble	Partially soluble
THF	Insoluble	Partially soluble
35% HCl	Soluble	Soluble
Toluene	Insoluble	Insoluble
NaOH (1%)	Insoluble	Partially soluble
Hexane	Insoluble	Insoluble
Acetic acid	Soluble	Partially soluble
DMF	Insoluble	Soluble

3.5. X-ray diffraction

X-ray diffraction spectra of chitosan, *N*-naphthaloyl chitosan and chitosan biopolymer dye are shown in Fig. 5. X-ray diffraction studies of chitosan (Fig. 5a) exhibits very broad peaks at $2\theta = 10^\circ$ and $2\theta = 20^\circ$. Chitosan shows very broad lines especially for the smaller diffraction angles, thereby indicating that long range disorder is found in polymer samples. The broader small angle peaks in chitosan suggests that *N*-naphthaloyl chitosan exhibits higher long range order. Diffractive region of *N*-Naphthaloyl chitosan (Fig. 5b) is observed at 2θ of 3°, 8°, 12°, 16°, 19°, and broad peak at 26.5°. The main diffractive region of chitosan polymer dye (Fig. 5c) is at 2θ of 3°, 7.8°, 12°, 19° and 26.35°. The absence of intense peaks at $2\theta = 10^\circ$ and $2\theta = 20^\circ$ attributed to chitosan are indicatives of chitosan scarcity as crystalline phase. Chitosan polymer dye has higher lower intensity pattern than chitosan which indicates that the chitosan polymer dye is substantially more amorphous due to disruption of hydrogen bonding.

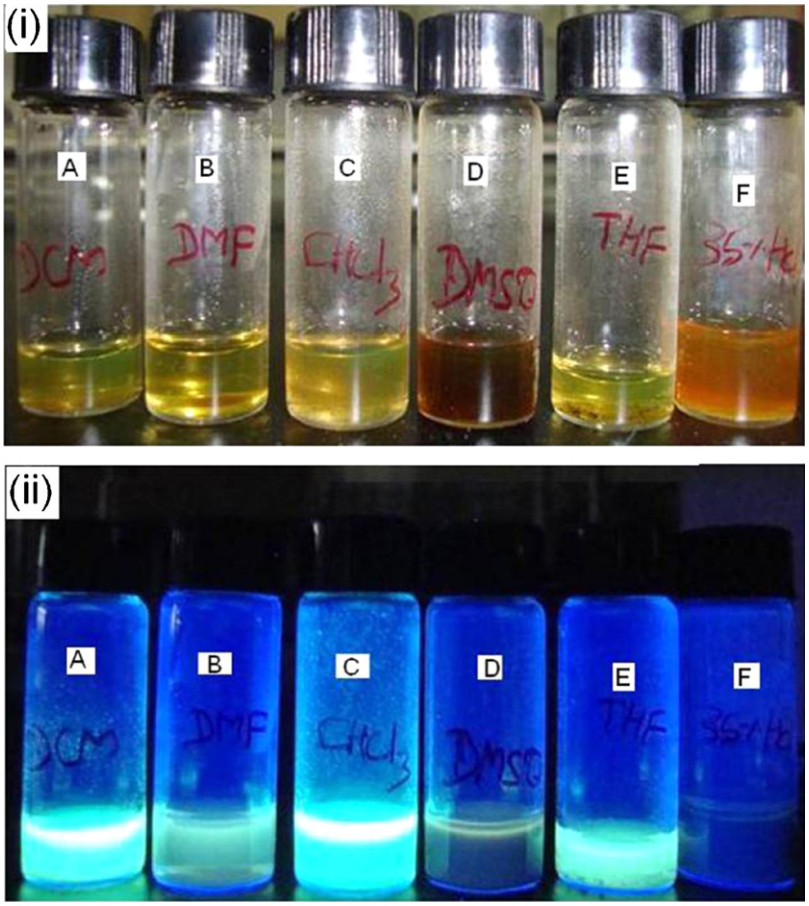

Fig. 7. Photographs of chitosan biopolymer dye (i) white light and (ii) UV light in (A) DCM, (B) DMF, (C) $CHCl_3$, (D) DMSO, (E) THF, and (F) 35% HCl.

3.6. Surface morphology

The scanning electron micrographs images showed different surfaces of chitosan and chitosan biopolymer dye in Fig. 6. Chitosan had a nonporous and flat lamellar phase surface (Fig. 6A and B), while chitosan biopolymer dye had a complicated three dimensional structures (Fig. 6D). The SEM images of Fig. 6C and D, shows the highly porous interconnectivity of chitosan biopolymer dye (Wang et al., 2010).

3.7. Solubility test

The solubility of chitosan and chitosan biopolymer dye in organic and inorganic different solvents determined as shown in Table 1. Chitosan polymer backbone consists of hydrophilic group and is hydrophobic nature. It is usually only soluble in acidic solutions such as aqueous acidic solution by transferring in to ionic structure (Singh & Dutta, 2009). The insolubility of chitosan in aqueous and organic solvent has attributed to extensive intramolecular and intermolecular hydrogen bonding between the chain and sheets respectively in crystalline structure (Nishimura, Kohgo, Kurita, & Kuzuhara, 1991). The solubility depends on the alkyl chain length and substituent of chitosan and chitosan biopolymer dye. The chitosan biopolymer dye was insoluble in water because of degree of substitution due to an increase in hydrophobicity (Kumar & Koh, 2012). The solubility of chitosan biopolymer dye is confirmed in Fig. 7 showed the photographs of (i) white light and (ii) UV light in (A) DCM, (B) DMF, (C) $CHCl_3$, (D) DMSO, (E) THF, and (F) 35% HCl. The chitosan biopolymer dye with increased solubility in organic solvents was due to insertion of more hydrophilic group regardless of the DS. The solubility data, which open new perspectives for the employment of chitosan biopolymer dye material in biosensor and the field of biomedical applications.

3.8. UV–vis absorption spectroscopy

The UV–vis absorption spectrum of pure chitosan in 1% acetic acid was 215 nm (Kumar et al., 2010), and chitosan biopolymer dye shows two maxima in the 260–300 nm regions and a wide absorption band with a maximum at 360 nm (Fig. 8). Comparison with the spectrum of chitosan biopolymer dye shows that introduction of a naphthalimide and fluoroquinolone ring in the acceptor

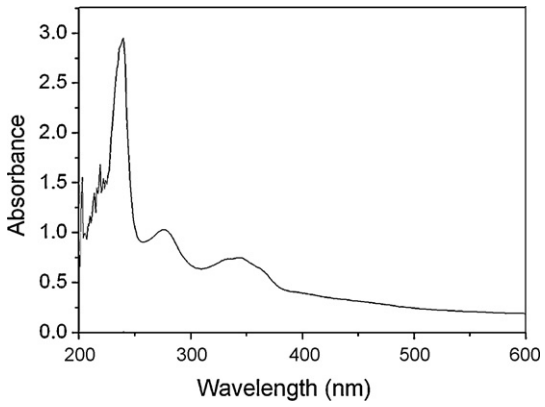

Fig. 8. UV–vis spectrum of chitosan biopolymer dye.

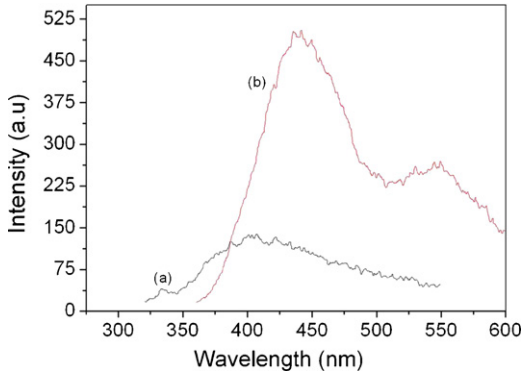

Fig. 9. PL spectra of chitosan (a) and chitosan biopolymer dye (b) at excitation wavelength of 325 nm.

block produces a red shift of the maximum of the chitosan band to 360 nm.

3.9. Photoluminescence (PL) study

The Photoluminescence spectra (PL) of the native chitosan and chitosan biopolymer dye are shown in Fig. 9. The emission spectra and fluorescent intensity of chitosan and chitosan biopolymer dye were performed at an excitation wavelength (λ_{ex}) of 325 nm. The emission spectra of pure chitosan (λ_{em}) broad peak at 425 nm and chitosan biopolymer dye λ_{em} broad peak at 442 nm and 551 nm at excitation wavelength (λ_{ex}) of 325 nm. Chitosan biopolymer dye showed red-shift emission maxima due to the introduction of side chain and the electronic effect of the substituent on the side chain, because of the attachment of the naphthalimide with fluoroquinolone side group to the backbone will enlarge the degree of delocalized π-bond on the electron rich polymer main chain (Kumar, Dutta, & Koh, 2011). Naphthalimide is strongly electron withdrawing, the piperazine nitrogen that links to the C-4 position of the naphthalimide ring. The naphthalimide and fluoroquinolone moity are two acceptor units, which exist by the sides of the piperazine ring. Different polarity of solvents showed that the photo-induced energy transfer process was accelerated in polar solvents, which led to a lower fluorescence quantum yield (Hu, Wang, & Su 2008).

4. Conclusions

A new chitosan biopolymer dye containing naphthalimide with fluoroquinolone moieties was synthesized. The synthetic strategy is straightforward, benefits from high yield and eco-friendly. The structure was confirmed by ^{1}H NMR, FTIR, FT-Raman, and XRD spectroscopy. The TGA and DSC studies showed that the biopolymer dye is thermally stable. The SEM images showed chitosan biopolymer dye had porous interconnected surface. The solubility of synthesized material was in different organic and inorganic solvents. UV–visible and photoluminescence (PL) showed red shift maxima. Overall, the results showed that the chitosan biopolymer dye could widen the practical applications in the field of optical and biosensing.

Acknowledgment

This research was supported by the 2012 KU Brain Pool Programme of Konkuk University, Seoul, South Korea.

References

Bojinov, V., Ivanova, G., & Simeonov, D. (2004). Synthesis and photophysical investigations of novel polymerizable blue emitting fluorophores combination of a hindered amine with a benzo[de]isoquinoline-1,3-dione. *Macromolecular Chemistry and Physics*, *9*, 1259–1268.

Coya, C., Alvarez, A. L., Ramos, M., Gomez, R., Seoane, C., & Segura, J. L. (2012). Highly efficient solution processed white organic light-emitting diodes based on novel copolymer single layer. *Synthetic Metals*, *161*, 2580–2584.

Dizman, B., Elasri, M. O., & Mathias, L. J. (2005). Synthesis, characterization, and antibacterial activities of novel methacrylate polymers containing norfloxacin. *Biomacromolecules*, *6*, 514–520.

Ghassemi, H., & Hay, A. S. (1993). Novel poly (ether imide)s utilizing hydrazine as the diamine. *Macromolecules*, *26*, 5824–5826.

Hu, Y., Wang, B., & Su, Z. (2008). Synthesis and photophysical properties of a novel green fluorescent polymer for Fe^{3+} sensing. *Polymer International*, *57*, 1343–1350.

Huang, X. M., Fang, Y., Li, X., Xie, Y. S., & Zhu, W. H. (2011). Novel dyes based on naphthalimide moiety as electron acceptor for efficient dye-sensitized solar cells. *Dyes and Pigments*, *90*, 297–303.

Ifuku, S., Miwa, T., Morimoto, M., & Saimoto, H. (2011). Preparation of highly chemoselective *N*-phthaloyl chitosan in aqueous media. *Green Chemistry*, *13*, 1499–1502.

Jang, J., Bae, J., & Park, E. (2006). Polyacrylonitrile nanofibers: Formation mechanism and applications as a photoluminescent material and carbon-nanofiber precursor. *Advanced Functional Materials*, *16*, 1400–1406.

Katritzky, A. R., & Narindoshvili, T. (2008). Chiral peptide nucleic acid monomers (PNAM) with modified backbones. *Organic and Biomolecular Chemistry*, *6*, 3171–3176.

Katsarou, M. E., Efthimiadou, E. K., Psomas, G., Karaliota, A., & Vourloumis, D. (2008). Novel copper (II) complex of *N*-propyl-norfloxacin and 1,10-phenanthroline with enhanced antileukemic and DNA nuclease activities. *Journal of Medicinal Chemistry*, *51*, 470–478.

Kim, K., Kwon, S., Park, J. H., Chung, H., Jeong, S. Y., & Kwon, I. C. (2005). Characterisations of size-controlled self-aggregates based on glycol chitosans modified with deoxycholic acid. *Biomacromolecules*, *6*, 1154–1158.

Kumar, S., Dutta, P. K., & Koh, J. (2011). A physico-chemical and biological study of novel chitosan-chloroquinoline derivative for biomedical applications. *International Journal of Biological Macromolecules*, *49*, 356–361.

Kumar, S., & Koh, J. (2012). Physiochemical and optical study of chitosan-terephthaldehyde derivative for biomedical applications. *International Journal of Biological Macromolecules*, *51*, 1167–1172.

Kumar, S., Koh, J., Kim, H., Gupta, M. K., & Dutta, P. K. (2012). A new chitosan–thymine conjugate: Synthesis, characterization and biological activity. *International Journal of Biological Macromolecules*, *50*, 493–502.

Kumar, S., Nigam, N., Ghosh, T., Dutta, P. K., Yadav, R. S., & Pandey, A. C. (2010). Preparation, characterization and optical properties of a chitosan-anthraldehyde crosslinkable film. *Journal of Applied Polymer Science*, *115*, 3056–3062.

Lee, M. H., Han, J. H., Kwon, P. S., Bhuniya, S., Kim, J. Y., Sessler, J. L., et al. (2012). Hepatocyte-targeting single galactose appended naphthalimide: A tool for intracellular thiol imaging in vivo. *Journal of the American Chemical Society*, *134*, 1316–1322.

Lim, C. K., Kim, S., Kwon, I. C., Ahn, C. H., & Park, S. Y. (2009). Dye-condensed biopolymeric hybrids: Chromophoric aggregation and self-assembly toward fluorescent bionanoparticles for near infrared bioimaging. *Chemistry of Materials*, *21*, 5819–5825.

Lim, C. K., Shin, J., Kwon, I. C., Jeong, S. Y., & Kim, S. (2012). Iodinated photosensitizing chitosan: Self-assembly into tumor-homing nanoparticles with enhanced singlet oxygen generation. *Bioconjugate Chemistry*, *23*, 1022–1028.

Mazuel, C. (1991). Norfloxacin. In K. Florey (Ed.), *Analytical profiles of drug substances*, (pp. 557–600). San Diego: Academic Press.

Michalet, X., Pinaud, F. F., Bentolila, L. A., Tsay, J. M., Doose, S., Li, J. J., et al. (2005). Quantum dots for live cells, in vivo imaging, and diagnostics. *Science*, *307*, 538–544.

Muzzarelli, R. A. A. (1977). *Chitin*. Oxford, UK: Pergamon Press.

Muzzarelli, R. A. A., Boudrant, J., Meyer, D., Manno, N., DeMarchis, M., & Paoletti, M. G. (2012). Current views on fungal chitin/chitosan, human chitinases, food preservation, glucans, pectins and inulin: A tribute to Henri Braconnot, precursor of the carbohydrate polymers science, on the chitin bicentennial. *Carbohydrate Polymers*, *87*, 995–1012.

Muzzarelli, R. A. A., & Muzzarelli, C. (2005). Chitosan chemistry: Relevance to the biomedical sciences. In T. Heinze (Ed.), *Advances in polymer science* (pp. 151–209). Berlin: Springer Verlag.

Nishimura, S. I., Kohgo, O., Kurita, K., & Kuzuhara, H. (1991). Chemospecific manipulations of a rigid polysaccharide syntheses of novel chitosan derivatives with excellent solubility in common organic solvents by regioselective chemical modifications. *Macromolecule*, *24*, 4745–4748.

Sahoo, S., Chakraborti, C. K., Mishra, S. C., Nanda, U. N., & Naik, S. (2011). FTIR and XRD investigations of some fluoroquinolones. *International Journal of Pharmacy and Pharmaceutical Sciences*, *3*, 165–170.

Saksena, B. D. (1938). Raman spectra of some organic bicyclic compounds. *Proceeding of the Indian Academy of Sciences A*, *8*, 73–100.

Satoh, T., Vladimirov, L., Johmen, M., & Sakairi, N. (2003). Preparation and thermal dehydration of *N*-(carboxy)acyl chitosan derivatives with high stereoregularity. *Chemistry Letters*, *32*, 318–319.

Seydack, M. (2005). Nanoparticle labels in immunosensing using optical detection methods. *Biosensors and Bioelectronics*, *20*, 2454–2469.

Singh, J., & Dutta, P. K. (2009). Preparation, circular dichroism induced helicle conformation and optical property of chitosan acid salt complexes for biomedical applications. *International Journal of Biological Macromolecules*, *45*, 384–392.

Socrates, G. (2001). *Infrared and Raman characteristic group frequencies: Tables and charts* (3rd ed.). England: Wiley.

Son, G. S., Yeo, J. A., Kim, M. S., Kim, S. K., Holmen, A., Akerman, B., et al. (1998). Binding mode of norfloxacine to calf thymus DNA. *Journal of the American Chemical Society*, *120*, 6451–6457.

Wang, G., Ao, Q., Gong, K., Wang, A., Zheng, L., Gong, Y., et al. (2010). The effect of topology of chitosan biomaterials on the differentiation and proliferation of neural stem cells. *Acta Biomaterialia*, *6*, 3630–3639.

Wang, Q., Li, C., Zou, Y., Wang, H., Yi, T., & Huang, C. (2012). A highly selective fluorescence sensor for Tin and its application in imaging live cells. *Organic and Biomolecular Chemistry*, *10*, 6740–6746.

Wang, X., Du, Y., Ding, S., Wang, Q., Xiong, G., Xie, M., et al. (2006). Preparation and third-order optical nonlinearity of self-assembled chitosan/CdSe–ZnS core–shell quantum dots multilayer films. *The Journal of Physical Chemistry B*, *110*, 1566–1570.

Yang, Y., Cui, J., Zheng, M., Hu, C., Tan, S., Xiao, Y., et al. (2012). One-step synthesis of amino-functionalized fluorescent carbon nanoparticles by hydrothermal carbonization of chitosan. *Chemical Communications*, *48*, 380–382.

Zhang, J. F., Kim, S. J., Han, H., Lee, S. J., Pradhan, T., Cao, Q. Y., et al. (2011). Pyrophosphate selective fluorescent chemosensor based on 1,8-naphthalimide–DPA–Zn(II) complex and its application for cell imaging. *Organic Letters*, *13*, 5294–5297.

Zhang, K., Geissler, A., Fischer, S., Brendler, E., & Baucker, E. (2012). Solid-state spectroscopic characterization of α-chitins deacetylated in homogeneous solutions. *The Journal of Physical Chemistry B*, *116*, 4584–4592.

Zhang, Y., Zhu, W., Wang, W., Tian, H., Su, J., & Wang, W. (2002). Synthesis and nonlinear optical properties of rod-like luminescent materials containing Schiff base and naphthalimide units. *Journal of Materials Chemistry*, *12*, 1294–1300.

Zhu, W., Minami, N., Kazaoui, S., & Kim, Y. (2003). Fluorescent chromophore functionalized single-wall carbon nanotubes with minimal alteration to their characteristic one-dimensional electronic states. *Journal of Materials Chemistry*, *13*, 2196–2201.